



Short-term exposure to high relative humidity increases blood urea and influences colonic urea-nitrogen metabolism by altering the gut microbiota

Hongmei Yin^{a,1}, Yadong Zhong^{a,1}, Hui Wang^a, Jielun Hu^{a,*}, Shengkun Xia^a, Yuandong Xiao^c, Shaoping Nie^a, Mingyong Xie^{a,b,*}

^a State Key Laboratory of Food Science and Technology, China-Canada Joint Lab of Food Science and Technology (Nanchang), Nanchang University, 235 Nanjing East Road, Nanchang 330047, China

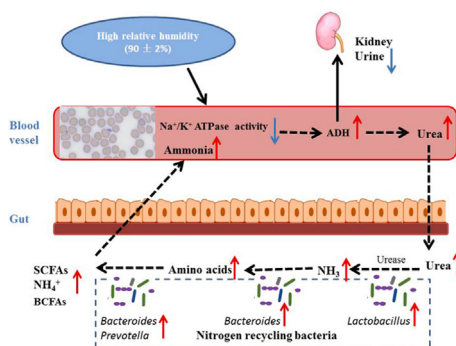
^b National R&D Center for Freshwater Fish Processing, Jiangxi Normal University, Nanchang, Jiangxi 330022, China

^c The College of National Land Resource and Environment, Jiangxi Agriculture University, Nanchang, Jiangxi 330045, China

HIGHLIGHTS

- Plasma urea was increased along with erythrocyte Na^+/K^+ -ATPase activity reduced and abnormal erythrocyte morphologies appeared during 14-day high relative humidity ($90 \pm 2\%$) exposure.
- Shortly after 12-h and 24-h exposures, urea influx and ammonia level were increased in the colon of mice, respectively.
- Colonic urea-nitrogen metabolism was influenced by the increased levels of ammonia, amino acids and short-chain fatty acids during 14-day exposure.
- Gut bacteria related to urease production, amino acids metabolism and SCFAs production was enriched during the exposure.

GRAPHICAL ABSTRACT



ARTICLE INFO

Article history:

Received 1 March 2021

Accepted 9 March 2021

Available online 15 March 2021

Keywords:

High relative humidity

Na^+/K^+ -ATPase

Urea

Colonic urea-nitrogen metabolism

Gut microbiota

ABSTRACT

Introduction: Colonic urea-nitrogen metabolites have been implicated in the pathogenesis of certain diseases which can be affected by environmental factors.

Objectives: We aimed to explore the influence of ambient humidity on colonic urea-nitrogen metabolism.

Methods: Blood biochemical indexes, metabolites of intestinal tract, and gut microbiota composition of mice ($n = 10/\text{group}$) exposed to high relative humidity (RH, $90 \pm 2\%$) were analyzed during the 14-day exposure.

Results: After 12-h exposure, plasma blood urea nitrogen (BUN) level increased along with a decrease in the activity of erythrocyte Na^+/K^+ -ATPase. Moreover, abnormal erythrocyte morphologies appeared after 3 days of exposure. The colonic BUN and ammonia levels increased significantly after the 12-h and 24-h exposure, respectively. The colonic level of amino acids, partly synthesized by gut microbiota using

Peer review under responsibility of Cairo University.

* Corresponding authors at: State Key Laboratory of Food Science and Technology, China-Canada Joint Lab of Food Science and Technology (Nanchang), Nanchang University, 235 Nanjing East Road, Nanchang 330047, China (M. Xie).

E-mail addresses: hujielun@ncu.edu.cn (J. Hu), myxie@ncu.edu.cn (M. Xie).

¹ These authors contributed equally to this work and should be considered co-first authors.

<https://doi.org/10.1016/j.jare.2021.03.004>

2090-1232/© 2021 The Authors. Published by Elsevier B.V. on behalf of Cairo University.

This is an open access article under the CC BY-NC-ND license (<http://creativecommons.org/licenses/by-nc-nd/4.0/>).

ammonia as the nitrogen source, was significantly higher on the 7th day. Furthermore, the level of fecal short-chain fatty acids was significantly higher after 3-day exposure and the level of branched-chain fatty acids increased on the 14th day. Overall, gut microbiota composition was continuously altered during exposure, facilitating the preferential proliferation of urea-nitrogen metabolism bacteria.

Conclusion: Our findings suggest that short-term high RH exposure influences colonic urea-nitrogen metabolism by increasing the influx of colonic urea and altering gut microbiota, which might further impact the host health outcomes.

© 2021 The Authors. Published by Elsevier B.V. on behalf of Cairo University. This is an open access article under the CC BY-NC-ND license (<http://creativecommons.org/licenses/by-nc-nd/4.0/>).

Introduction

Based on current greenhouse gas emissions, climatologists predict that in the coming century, the earth's climate would become both warmer and more humid [1]. Regrettably, an increase in humidity could be a direct or indirect trigger for several diseases [1]. Environmental epidemiology revealed that humidity was related to all-cause mortality and morbidity, involving cardiovascular, pulmonary, zoonotic, gastrointestinal, and urologic diseases [1]. However, the evidence relating the increase in humidity with the health impacts remains inconsistent. For example, no association between relative humidity and daily hemorrhagic and ischemic stroke counts were found in Hong Kong [2]. Likewise, humidity showed little or no added effect on heat-related mortality in Australia [3] and the United States [4]. It was suggested that to acknowledge the negative/positive impact of humidity related mortality under hot-dry or warm-humid climate, the health effects of temperature and humidity must be analyzed separately [5]. Moreover, overlooking humidity can result in a favorable impact on mortality than in actuality [6]. It was found that the relative humidity (RH) above 70% has a significant impact on human responses which gets further amplified with the increase in air temperature [7]. Notably, in many cities, such as Chongqing, Guangzhou, and Haikou in China, due to the strong precipitation in summer, the indoor humidity can reach above 70% [8]. Therefore, it is critical to study the health influences of high humidity detached from high temperature.

Gut microbiota and its metabolites affecting host physiology and metabolism are the crucial factors for host body homeostasis [9]. Ni *et al.* found that in patients with Crohn's disease, an increase in fecal amino acids content was positively correlated with disease activity, and for the mechanism, the gut microbiota dysbiosis was the promoting factor for bacterial urease-mediated change in nitrogen flux [10]. The disrupted intestinal microbiota composition and its metabolites might disrupt the intestinal barrier [11], which was related to inflammation, oxidative and nitrosative stress [12,13]. A multiple myeloma study suggested a similar mechanism, in which an increase in relative abundance of nitrogen-recycling bacteria accelerated the disease progression [14]. Urea, the major end-product of mammalian protein catabolism, passes from the circulation into the host's digestive tract to be broken down by bacterial urease into ammonia and carbon dioxide [15,16]. Ammonia, a potentially toxic metabolite, might have a direct toxic effect on colonic cells [17]. Besides, ammonia is the main nitrogen source for the synthesis of bacterial amino acids and nucleotides [18]. Furthermore, with the aid of gut microbiota, amino acids can be fermented into short-chain fatty acids (SCFAs) by deamination producing carboxylic acid and ammonia, or by decarboxylation producing an amine and carbon dioxide. Other than that, some toxic products, including amines, phenols/indoles, and sulfurous compounds, can also be produced during amino acid catabolism [19–21]. Notably, under higher thermal environments, the urea-nitrogen recycling in the lactating dairy cows was affected by the ambient temperature exhibiting a decrease in gut urea-N entry and an increase in urinary urea-N excretion [22]. Chen *et al.* [23] showed that 8 consecutive weeks of high humidity (85 ~ 90%, 12 h per day) at 30 ± 0.5 °C led to gut microbiota dysbiosis in mice.

However, the effect of a high humidity environment on urea-nitrogen metabolism involving gut microbiota is largely unknown.

Therefore, to examine the impact of short-term high humidity exposure in colonic urea-nitrogen metabolism, we constantly monitored gut microbiota, Na^+/K^+ -ATPase activity, the morphology of erythrocyte, plasma BUN, and colonic urea-nitrogen metabolism parameters including urea, ammonia, amino acids, and SCFAs during a 14-day study using a mice model. A man-made climate box maintaining normal temperature (23 ± 2 °C) and high RH ($90 \pm 2\%$) was used to expose the animals to the test environment.

Methods

Experimental animals

Male BALB/c mice (8 weeks old, 20 ± 2 g) were obtained from Vital River Laboratories (VRL, Beijing, China). The mice were acclimatized for 1 week under controlled temperature (23 ± 2 °C) and RH ($55 \pm 5\%$) in a 12/12 day/night cycle environment and fed a standard laboratory diet (VRL, Beijing, China). This study was approved by the Animal Care Review Committee (Animal application approval number 0064257) at Nanchang University, China.

Experimental design

As shown in Fig. 1, after environmental adaptation, all the animals were randomly divided into 6 groups ($n = 10$). Mice maintained under normal humidity ($55 \pm 5\%$) for 14 days were named the Normal group, and those exposed to high RH ($90 \pm 2\%$) in a man-made climate box (RXZ-500C-5, Ningbo Jiangnan instrument factory, China) for 12 h, 24 h, 3 days, 7 days and 14 days were named the 12 h group, 24 h group, 3 days group, 7 days group and 14 days group, respectively. Parameters such as body weight, and food and water intakes were measured daily. After fasting for 12 h, peripheral blood samples were collected in dipotassium EDTA tubes and the mice were sacrificed by cervical dislocation. Before that, feces and the colonic contents were also collected and stored at -80 °C for further studies.

Giemsa-stained peripheral blood smears

To prepare blood smears, a drop of anticoagulant blood sample was evenly spread on a clean and dry silicified glass slide. After drying at room temperature (RT), the blood smears were soaked in methanol for 15 min, air-dried at RT, stained in Giemsa dye for 30 s, and then restained in PBS buffer diluted Giemsa dye (2 ~ 3:1, v:v) for 1–3 min. Then, the slides were cleanly washed using distilled water, followed by quick drying in a 37 °C oven. Images were collected using an Aperio Digital Pathology Slide Scanners (Aperio LV1, Leica, USA).

Measurement of erythrocyte Na^+/K^+ -ATPase activity, plasma antidiuretic hormone, BUN, and ammonia levels

The anticoagulant blood samples were allowed to come to RT for 1 h. Then, these were centrifuged at $827 \times g$ for 20 min to sep-

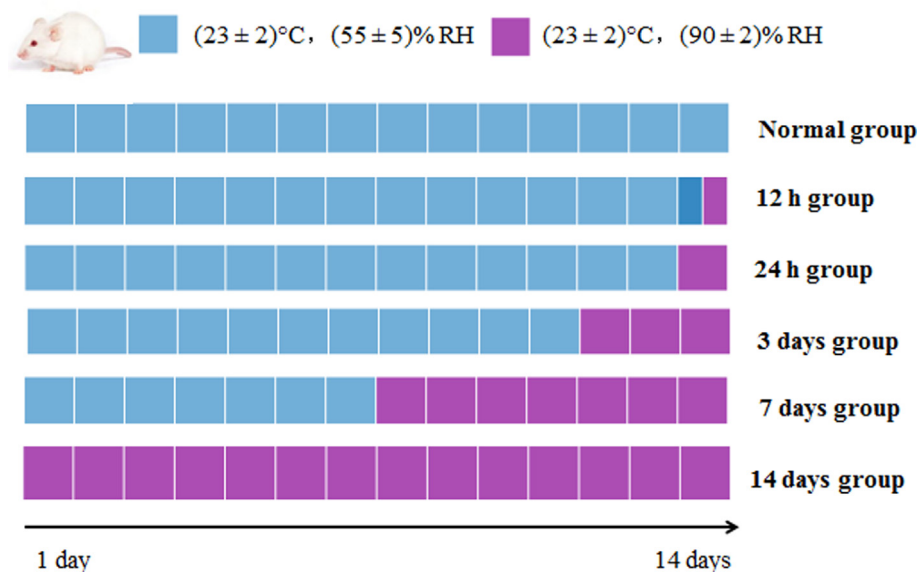


Fig. 1. The design scheme of animal experiment. Each blue square indicated that the mice were exposed to normal RH (55 ± 5%) for one day, while the purple one indicated that the mice were exposed to high RH (90 ± 2%) for one day. *Abbreviation:* RH, relative humidity.

arate the plasma supernatant and blood cells in the precipitate. To prepare a transparent and uniform hemolytic solution, the blood cells (100 μ L) were transferred into a new centrifuge tube and diluted by mixing with 4900 μ L pre-cooled distilled water. Lastly, the erythrocyte Na^+/K^+ -ATPase activity of the hemolytic solutions, the plasma BUN and ammonia levels were measured using the commercially available kits (Nanjing Jiancheng Bioengineering Institute, Jiangsu, China), following the manufacturer's instructions. The plasma antidiuretic hormone (ADH) content was measured by a commercial ELISA kit (Shanghai Enzyme-linked Biotechnology Co., Ltd., Shanghai, China).

Determination of colonic BUN and ammonia levels

The colonic content sample (10 mg) mixed with 990 μ L ultra-pure water was homogenized by a grinder (KZ-II, Servicebio, Wuhan, China). The mixture was centrifuged at $9184 \times g$ for 10 min. The supernatant was used to determine the BUN and ammonia levels using the commercially available kits (Nanjing Jiancheng Bioengineering Institute, Jiangsu, China) as per their protocols.

Analysis of fecal free amino acids content

Free amino acids were measured as described by Xiao *et al.* [24] with slight modifications. Briefly, 50 mg feces sample was mixed with 500 μ L 0.01 M HCl by vortexing for 30 min. The mixture was centrifuged at $827 \times g$ for 10 min. To remove the large peptides, the obtained supernatants were incubated with 8% w/v sulfosalicylic acid (1:1) for 15 min. The mixture was again centrifuged ($827 \times g$, 20 min), the supernatants were filtered (0.22 μ m, MCE) and injected into the automatic amino acid analyzer (S-433D, Sykam, Germany).

pH measurements and fecal SCFAs quantification

The fecal pH values were determined using a pH meter (PHS-25, Shanghai Precision Scientific Instruments Company, China). For SCFAs extraction, 100 mg feces sample was placed in a 2 mL round-bottomed and stoppered tube in an ice-cold water bath. Then, 400 μ L deionized water was added, and to ensure proper

mixing, the tube was intermittently vortexed for 2 min. Then, the tube was allowed to stand in the ice-cold water bath for another 20 min and then centrifuged at $4800 \times g$ for 20 min at 4 °C. The supernatant was filtered (0.22 μ m, MCE) and analyzed with gas chromatography as described in Hu *et al.* [25].

Gut microbiota analysis

Feces DNA samples were prepared using a TIANamp stool DNA Kit (Tiangen biotech Beijing co., LTD, China). The extracted DNA samples were checked for quality and concentration by 1% agarose gel electrophoresis and ultraviolet spectroscopy (Nanodrop ND-1000, Thermo Electron Corporation, USA). The V4 hypervariable regions of the bacteria 16S rRNA gene were amplified by PCR using primers 515F (5'-barcode-GTGCCAGCMGCCGCGGTAA-3') and 806R (5'-GGACTACHVGGGTWTCTAAT-barcode-3') [26]. Final PCR products were purified to remove unincorporated nucleotides and primers using the Qiaquick PCR Purification kit (Qiagen, Germany). Purified amplicons were quantified by using Agilent 2100 Bioanalyzer (Agilent Technologies, USA) with the High Sensitivity DNA Kit (Chips Reagents) (Agilent Technologies, USA), and were subjected to paired-end sequencing (2 \times 250 bp) on an Illumina Miseq platform (Illumina Inc., San Diego, CA, USA) according to standard protocols. Quality filtering was performed using fastp with default settings. For downstream analysis, the retained reads with an average length of 225 bp were processed with the open-source bioinformatics pipeline Quantitative Insights into Microbial Ecology (QIIME) [27]. Chimeric sequences were removed by the Usearch method and the sequences, with a minimum of 97% sequence similarity, were grouped into operational taxonomic units (OTUs) by UCLUST. From each OTU, representative sequences (most abundant) were aligned using the Python nearest Alignment Space Termination (PyNAST), and taxonomy was assigned by the Greengenes database (v.13.8). For alpha diversity, the OTU table was rarefied at an even sampling depth of 7050 sequences/sample. Species richness was estimated using Chao1 and the number of observed species diversity was analyzed using Shannon. The sequencing data was submitted to 16S National Center for Biotechnology Information (NCBI)-derived database (<http://www.ncbi.nlm.nih.gov>, <http://rdp.cme.msu.edu>) under NCBI SRA ID PRJNA689911.

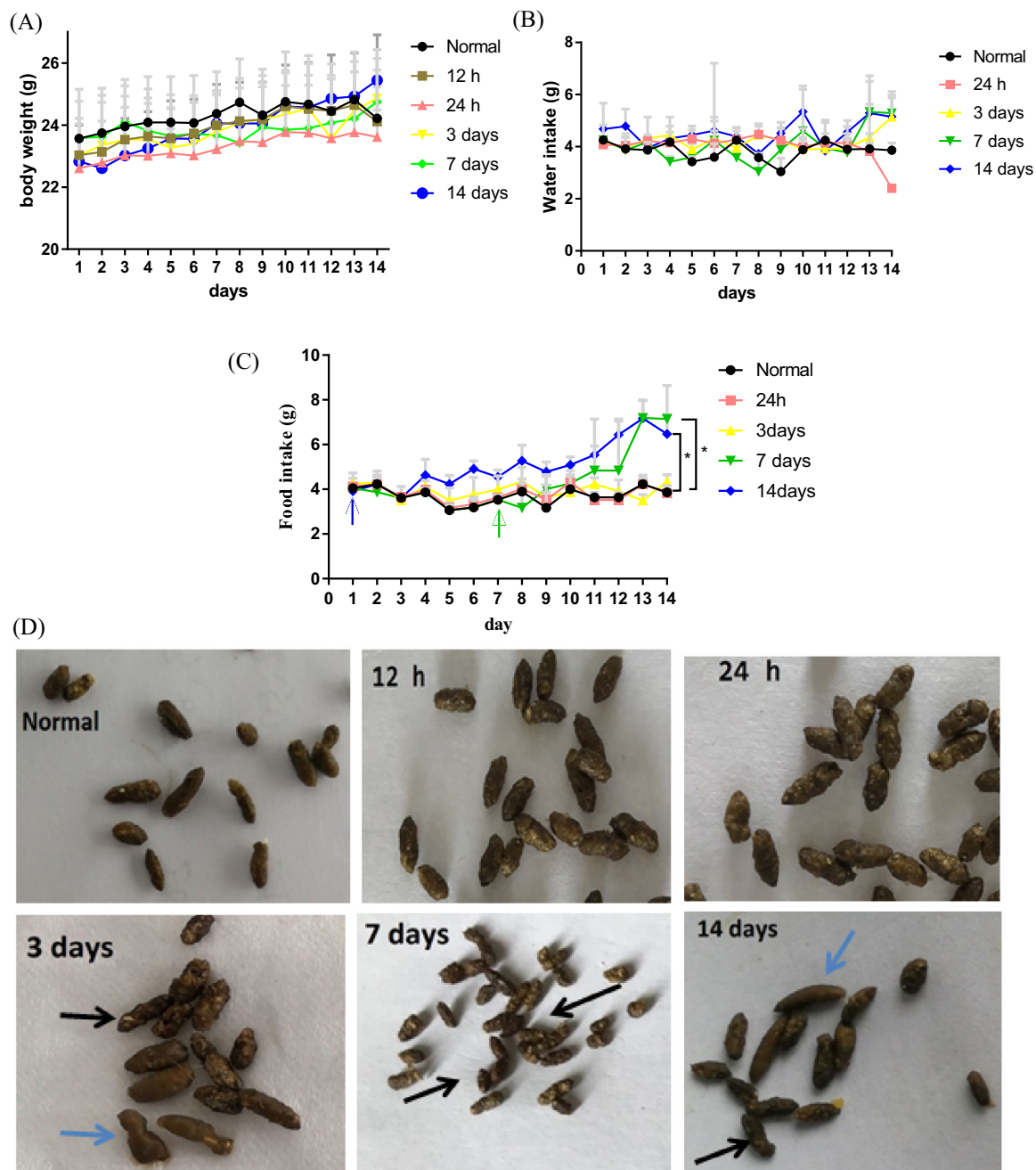


Fig. 2. The body weight (A), water (B) and food (C) intake of mice following 0 h (Normal), 12 h, 24 h, 3 days, 7 days and 14 days exposure to high RH ($n = 10$). The appearance of feces (D) showed its texture changed during the exposure. The black arrows indicate that the feces are dry and rough, while the blue arrows indicate that the feces contain high moisture content. Data is shown as mean \pm SD. * $p < 0.05$ are significantly different from the Normal group.

Statistics analysis

All results were subjected to statistical analysis by one-way ANOVA with the Least Significant Difference (LSD) test using SPSS 19.0 (SPSS Inc., Chicago, IL, USA). Difference in β -diversity was performed in R 3.6.0 by using bray-curtis metrics and packages of “vegan” and “ggplot2”. To analyze and visually display the relationship between gut microbiota data and other variables, Projection-to-Latent-Structures-Discriminant Analysis (PLS-DA) (SIMCA version 14, Umetrics, Umeå, Sweden) was applied. The correlation between different variables was performed in R 3.6.0 by using packages of “corrplot” and Pearson correlation analysis. Data

with * $p < 0.05$ and ** $p < 0.01$ were considered statistical significant, while $0.1 \geq p \geq 0.05$ were considered as tendency. All data are shown as mean \pm standard deviation (SD).

Results

Body weight, food intake, water consumption, and appearance of feces

During the high RH exposure, we did not observe any significant changes in body weight and water consumption (Fig. 2 A and B). However, the food intake was significantly increased only in the 7 days and 14 days groups when compared with the Normal group

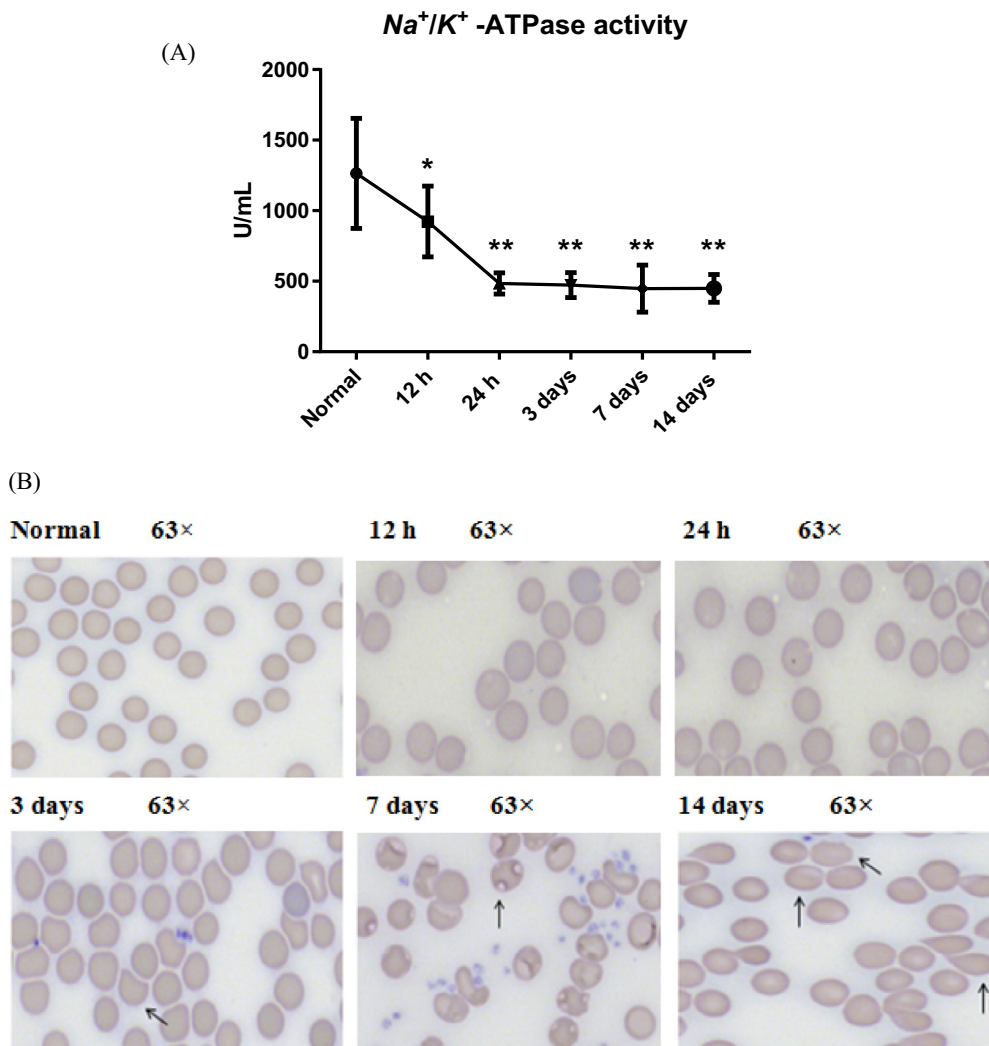


Fig. 3. The erythrocyte Na⁺/K⁺-ATPase activity (A) and Giemsa-stained peripheral blood smears (B) of mice following 0 h (Normal), 12 h, 24 h, 3 days, 7 days and 14 days exposure to high RH (n = 10). The arrows indicate abnormal erythrocyte morphology. Data is shown as mean ± SD. Compared with the Normal group, * p < 0.05 and ** p < 0.01 are taken as significantly different and extremely significant, respectively. Representative images were taken with 63 × magnifications.

(p < 0.05, Fig. 2 C). Meanwhile, the appearance of feces was inconsistent after 3-day exposure, which was dry and rough or wet in both the 3 days and 14 days groups while rough and dry in the 7 days group (Fig. 2 D).

Erythrocyte Na⁺/K⁺ -ATPase activity and erythrocyte morphology

Interestingly, compared to the Normal group that did not receive any high RH exposure, the erythrocyte Na⁺/K⁺ -ATPase activity in mice exposed to high RH exposure was markedly decreased (p < 0.05), even in the 12 h group. Moreover, the activity was further reduced (p < 0.01) and then remained stable after 3-days of high RH exposure (Fig. 3 A). Based on the remarkable reduction in Na⁺/K⁺ -ATPase activity, we next tested the mice's red blood cells for morphology by Giemsa staining (Fig. 3 B). Following the evaluation standard of peripheral blood smear [28], the erythrocyte morphology in the Normal group was smooth, round-shaped, and uniform size. Compared to the Normal group, the erythrocyte in the 12 h and 24 h groups were a little bit bigger. Notably, the erythrocyte size in the 3 days group was even bigger and exhibited a deformed shape. In the 7 days group, a bite gap appeared in some cells (belong to fragmented cells), which made

these bizarre red cells distinct from other cells. After 14-day of exposure, besides bite cells, burr cells and teardrop cells also appeared.

Plasma ADH, BUN and ammonia, and colonic BUN and ammonia levels

We observed that compared to the non-treated Normal group, the plasma ADH content increased with the duration of high RH exposure (Fig. 4 A), showing a significant change in both the 3 days and the 7 days groups (p < 0.05), and an extremely significant change in the 14 days group (p < 0.01). The increased ADH was accompanied by an increase in plasma BUN levels (p < 0.01), which leveled off after 24 h of exposure, as compared to the Normal group (Fig. 4 B). Notably, the difference in plasma ammonia contents between the exposure groups and the Normal group were insignificant. Even then, the plasma ammonia content in the 14 days group was higher than the 12 h (p < 0.05) and 7 days groups (p = 0.068) (Fig. 4 C).

Compared with the Normal group, the colonic BUN level was significantly higher in the 12 h (p < 0.01), 24 h (p < 0.05), and 3 days (p < 0.01) groups, while no change was noticed in the 7 days and 14 days groups (Fig. 4 D). Similarly, the colonic ammonia level was

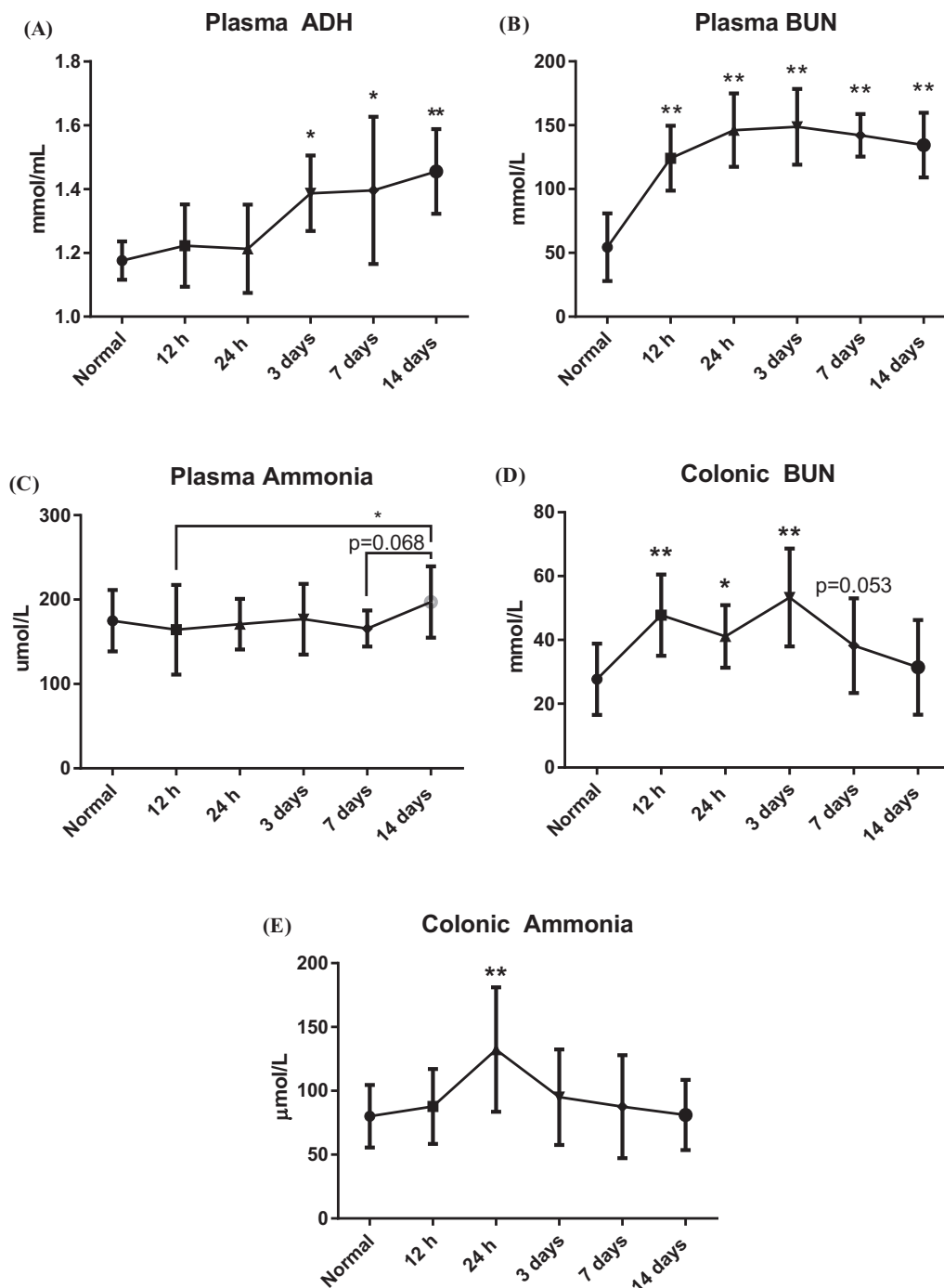


Fig. 4. The contents of plasma ADH (A), plasma BUN (B), plasma ammonia (C), colonic BUN (D) and colonic ammonia (E) of mice following 0 h (Normal), 12 h, 24 h, 3 days, 7 days and 14 days exposure to high RH ($n = 10$). Data is shown as mean \pm SD. Compared with the Normal group, * $p < 0.05$ and ** $p < 0.01$ are taken as significantly different and extremely significant, respectively. Abbreviations: ADH, antidiuretic hormone; BUN, Blood Urea Nitrogen; RH, relative humidity.

significantly higher ($p < 0.01$) in the 24 h group ($p < 0.01$, Fig. 4 E) than the Normal group. Surprisingly, no increase in ammonia level in colon content was noticed in the 3, 7, and 14 days groups.

Fecal free amino acids profile

A total of sixteen kinds of amino acids were tested for fecal free amino acids profile. We found that compared to the Normal group, the levels of free amino acids were higher in the 7 days group (Fig. 5 B). Meanwhile, an increase in the total free amino acid (Fig. 5 A) in the 7 days group ($p < 0.05$) showed significantly higher levels of isoleucine ($p < 0.05$), followed by the increase in leucine

($p = 0.068$) and phenylalanine ($p = 0.098$). Especially, the amino acids that can produce acetate (glycine, alanine, threonine, glutamate, lysine, and aspartate), butyrate (glutamate and lysine), and propionate (alanine and threonine) were increased in the 7 days group (Fig. 5 C).

Fecal SCFAs and pH values

The fecal pH values in the 12 h and 24 h groups were higher than the Normal group, and then showed a significant reduction ($p < 0.05$) in the 14 days group compared to the Normal group (Fig. 6 A). Accordingly, the total SCFAs levels increased with time

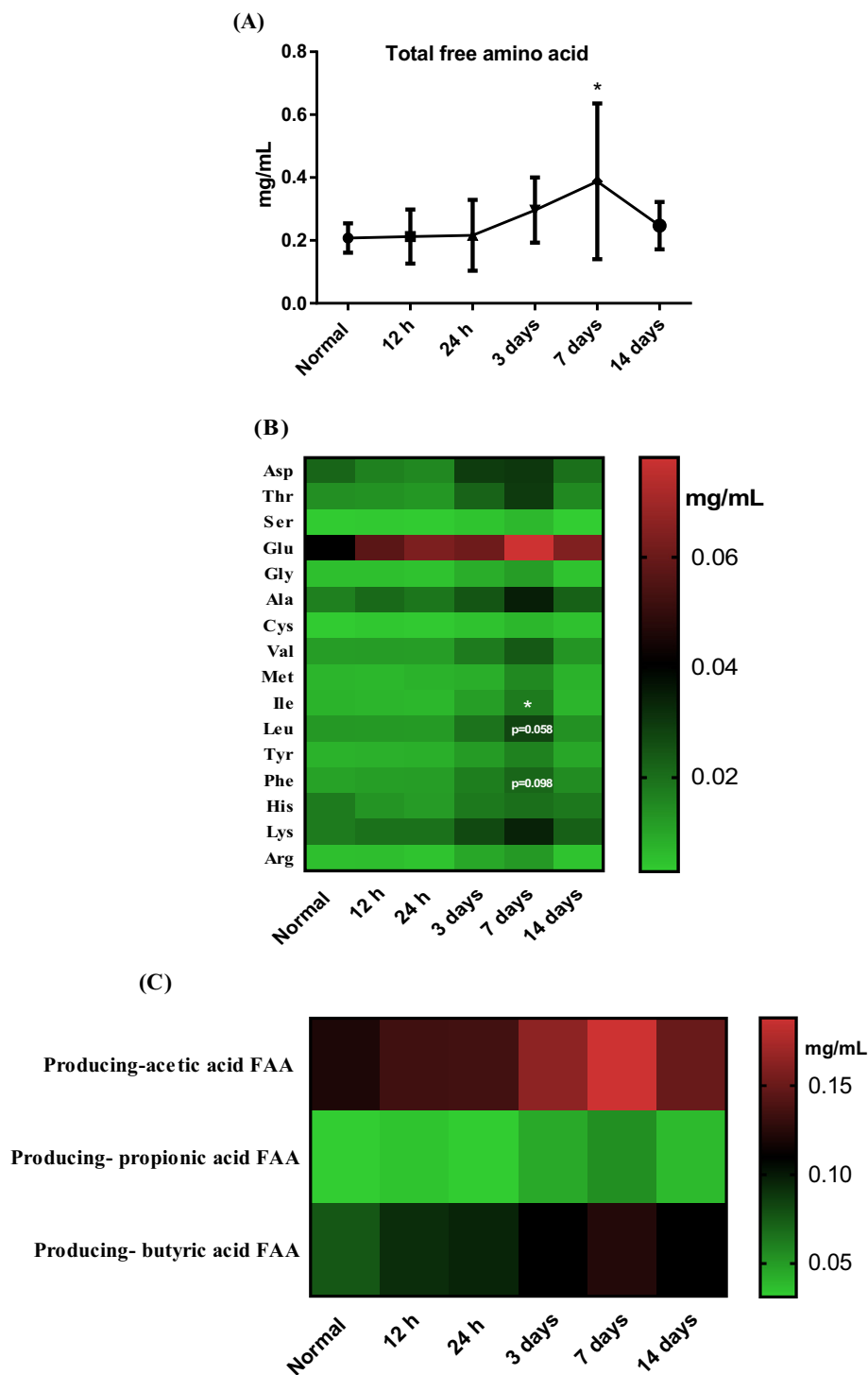


Fig. 5. The total free amino acid content (A), free amino acid profile (B) and producing acetic acid (Gly, Ala, Thr, Glu, Lys and Asp), propionic acid (Ala and Thr), butyric acid (Glu and Lys) free amino acid content (C) in feces of mice following 0 h (Normal), 12 h, 24 h, 3 days, 7 days and 14 days exposure to high RH ($n = 10$). Data is shown as mean \pm SD. * $p < 0.05$ are significantly different from the Normal group. *Abbreviation:* Asp, aspartic acid; Thr, threonine; Ser, serine; Glu, glutamic acid; Gly, glycine; Ala, alanine; Cys, cysteine; Val, valine; Met, methionine; Ile, isoleucine; Leu, leucine; Tyr, tyrosine; Phe, phenylalanine; His, histidine; Lys, lysine; Arg, arginine; RH, relative humidity.

and were significantly higher in the 3 days and the 7 days groups ($p < 0.05$). Notably, the increase in SCFAs levels was extremely significant in the 14 days group compared to the Normal group ($p < 0.01$, Fig. 6 B). Moreover, in the 14 days group, the contents of acetic acid ($p < 0.01$), butyric acid ($p < 0.05$), and propionic acid ($p < 0.01$) were raised significantly, along with the extreme increase in branched-chain fatty acids (BCFAs), i.e., isovaleric acid and isobutyric acid than in the Normal group ($p < 0.01$, Fig. 6 C).

Composition of fecal microbiota

α -diversity and β -diversity

The tested α -diversity indices included species richness indices (Chao1 and Observed OTUs) and species diversity indices (Shannon). Compared with the Normal group, the index of Shannon

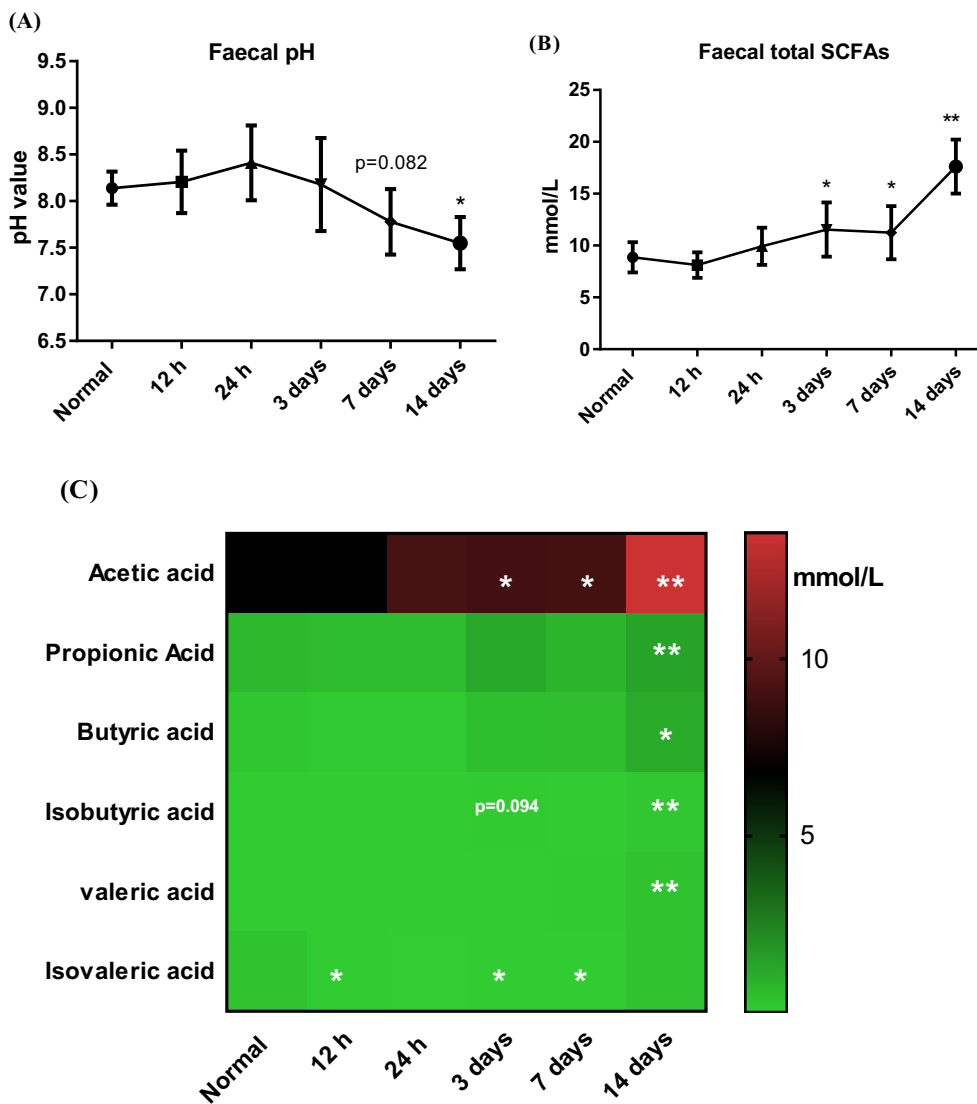


Fig. 6. The pH value (A), total SCFAs (B) and changes of SCFAs profile (C) in feces of the Normal, 12 h, 24 h, 3 days, 7 days and 14 days groups (*n* = 10). Data is shown as mean ± SD. Compared to the Normal group, * *p* < 0.05 and ** *p* < 0.01 are taken as significant and extremely significant, respectively. Abbreviations: SCFAs, short-chain fatty acid.

decreased significantly in all the exposure groups (except for the 14 days group) (*p* < 0.01, Fig. 7 B), and the index of Observed OTUs decreased in the 24 h and 3 days groups (Fig. 7 C, *p* = 0.056, *p* < 0.05, respectively). However, among groups, the Chao1 index remained almost the same (Fig. 7 A).

To explore the comprehensive microbial phenotypes of the Normal and high RH exposure groups, β-diversity analysis based on bray-curtis metrics was performed. We found that the exposure groups could be distinguished from the Normal group (Fig. 7 D). Adonis test confirmed that the β-diversity of the 24 h, 3, 7, and 14 days groups were significantly different from the Normal group (*p* = 0.0289, *p* = 0.0138, *p* = 0.0048 and *p* = 0.0091, respectively).

Phylum level

In the fecal samples, bacteria belonging to phylum Bacteroidetes, Firmicutes, Tenericutes, and Proteobacteria were detected (Fig. 8 A). Compared with the Normal group, the relative abundance of Bacteroidetes was significantly lower in the 24 h group (*p* < 0.05), while significantly higher in the 3 days (*p* < 0.01), 7 days (*p* < 0.05) and 14 days groups (*p* < 0.01, Fig. 8 B). However, the abundance of Firmicutes first increased in the 24 h group

(*p* < 0.05) relative to the Normal group, and then decreased in the 3 days (*p* < 0.01), 7 days (*p* < 0.05), and 14 days groups (*p* < 0.01) relative to the 24 h group (Fig. 8 C). This resulted in a higher Bacteroidetes-to-Firmicutes ratio in the 3 days (*p* < 0.01), 7 days (*p* < 0.05), and 14 days groups (*p* < 0.01) than that in the 24 h group (Fig. 8 D). Though a lower ratio of Bacteroidetes-to-Firmicutes was observed in the 24 h group than in the Normal group (*p* < 0.05). In all groups, phylum Tenericutes and Proteobacteria were in very low abundance and showed no significant difference among the groups (Fig. 8 E and F).

Family level

The microbiota composition at the family level is shown in Fig. 9 A. Compared with the Normal group, the relative abundance of S24-7 decreased significantly (*p* < 0.05), while the relative abundance of *Lactobacillaceae* increased significantly (*p* < 0.05) in the 24 h group (Fig. 9 B and D). Furthermore, compared to the 24 h group, the relative abundance of S24-7 increased significantly in the 3 days (*p* < 0.01) and 7 days groups (*p* < 0.05), while the relative abundance of *Lactobacillaceae* decreased significantly in the 3 days

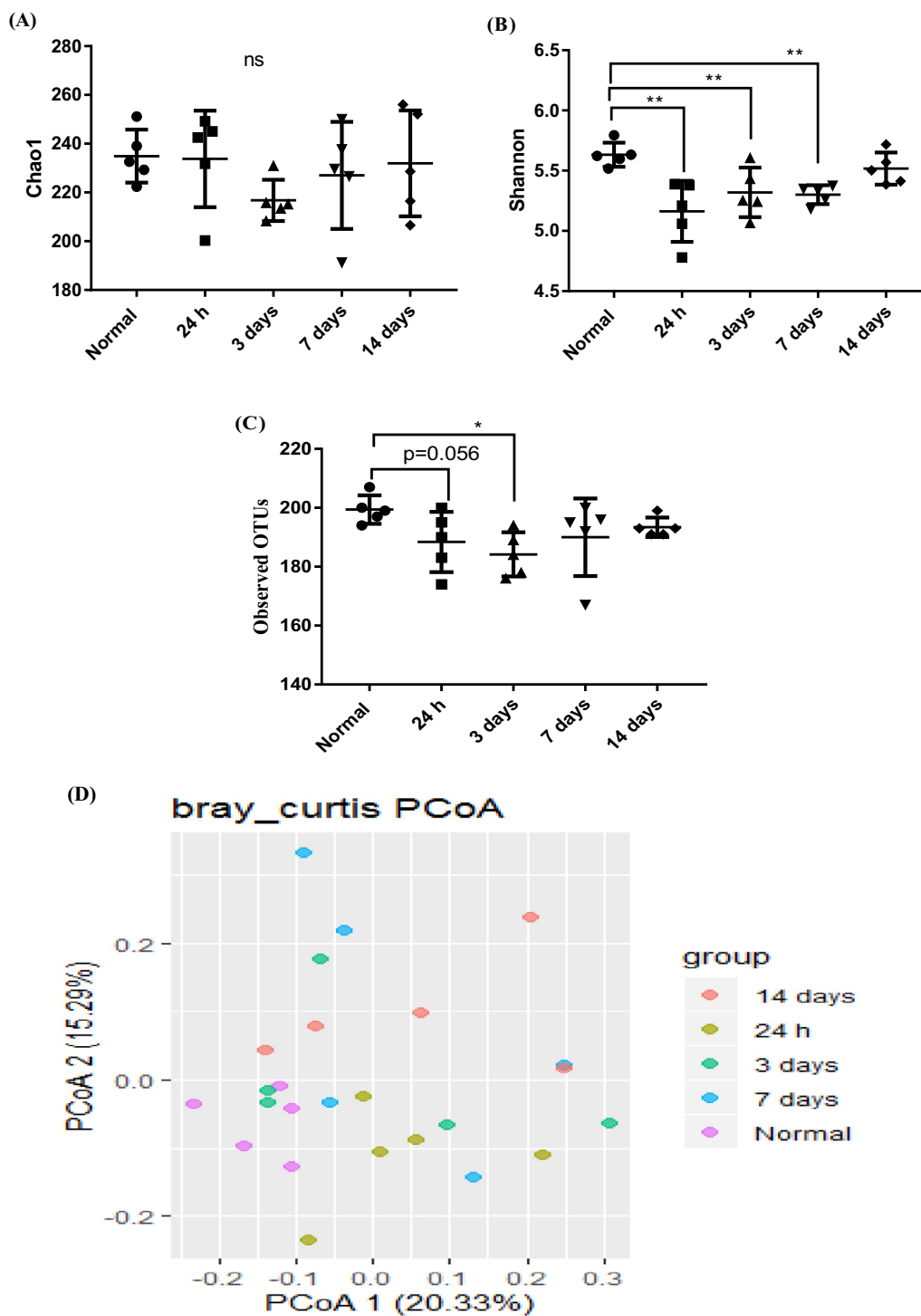


Fig. 7. Differential gut microbial characteristics in the Normal, 24 h, 3 days, 7 days and 14 days groups ($n = 5$). A-C) α -phylogenetic diversity (Chao1, Shannon and Observed OTUs) showed a lower α -diversity in groups of exposure to high RH than Normal group. Data is shown as mean \pm SD. * $p < 0.05$ and ** $p < 0.01$ are taken as significantly different and extremely significant, respectively. D) Principal co-ordinates analysis (PCoA) showed the 5 groups were separated clearly at the bray_curtis operational taxonomic units (OTU) level. Compared to the Normal group, the β -diversity of the 24 h, 3 days, 7 days and 14 days groups were significant different (Adonis test, $p = 0.0289$, 0.0138, 0.0048, and 0.0091, respectively). *Abbreviation:* ns, non-significant; RH, relative humidity.

($p < 0.05$), 7 days ($p < 0.05$) and 14 days groups ($p < 0.05$). Compared with the Normal group, the relative abundance of [*Odoribacteraceae*], *Clostridiaceae* and *Ruminococcaceae* were significantly lower in the high humidity exposure groups (Fig. 9 C, E, and F), while the relative abundance of *Erysipelotrichaceae* was significantly higher in the 24 h ($p < 0.05$) and 3 days ($p < 0.05$) groups (Fig. 9 G).

Genus level

Changes at the genus level are shown in Fig. 10. The dominant bacteria at the genus level included *Clostridiales_unclassified*, *S24-7_unclassified*, *Bacteroides*, *Rikenellaceae_unclassified*, *Prevotella*, *Bacteroidales_Paraprevotellaceae_Prevotella*, and *Coprococcus et al.*

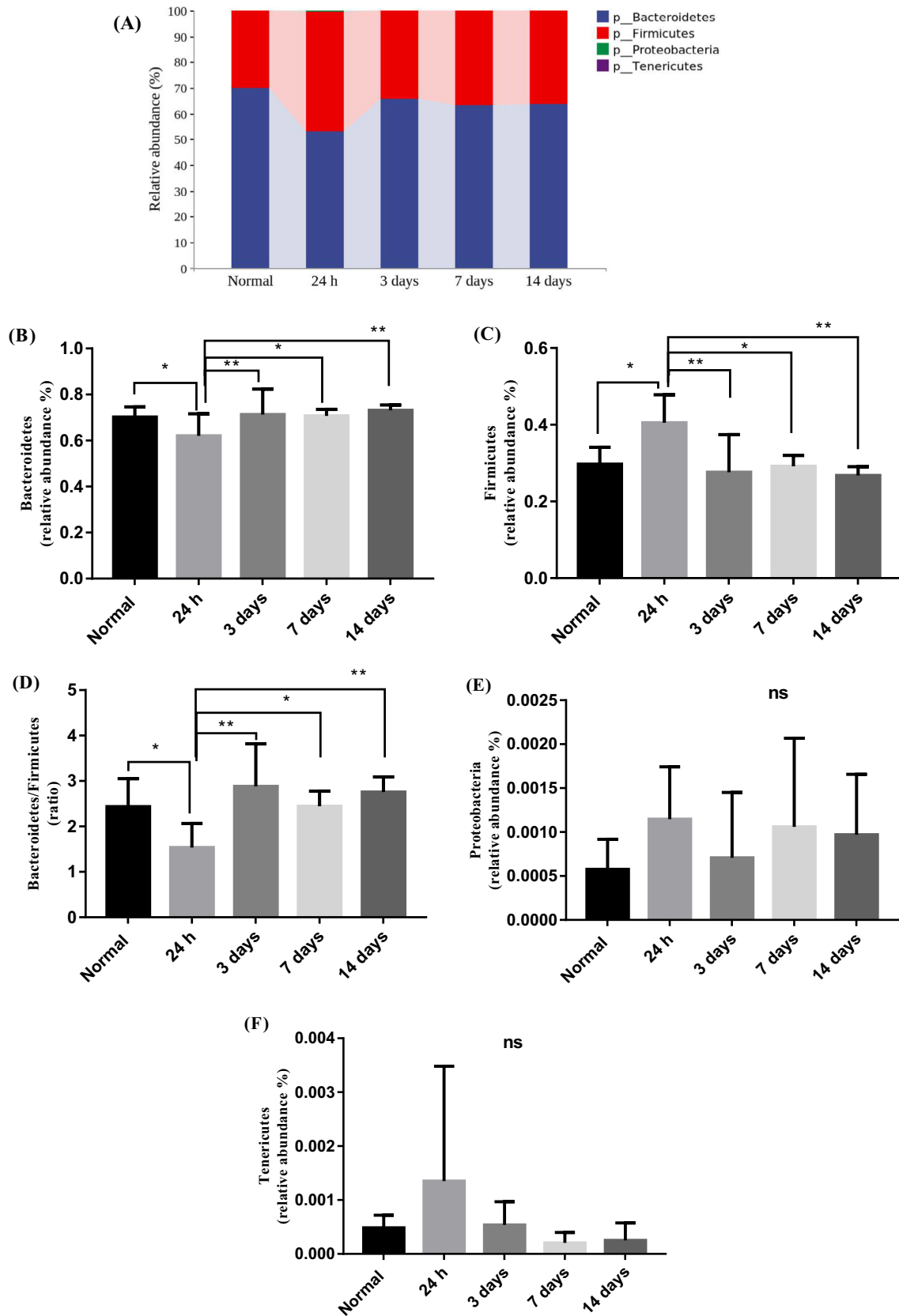


Fig. 8. Fecal microbiota composition at phylum level (A) and differences of bacterial relative abundance among 5 groups (B-F), $n = 5$. Data is shown as mean \pm SD. * $p < 0.05$ and ** $p < 0.01$ are taken as significant and extremely significant, respectively. Abbreviation: ns, non-significant.

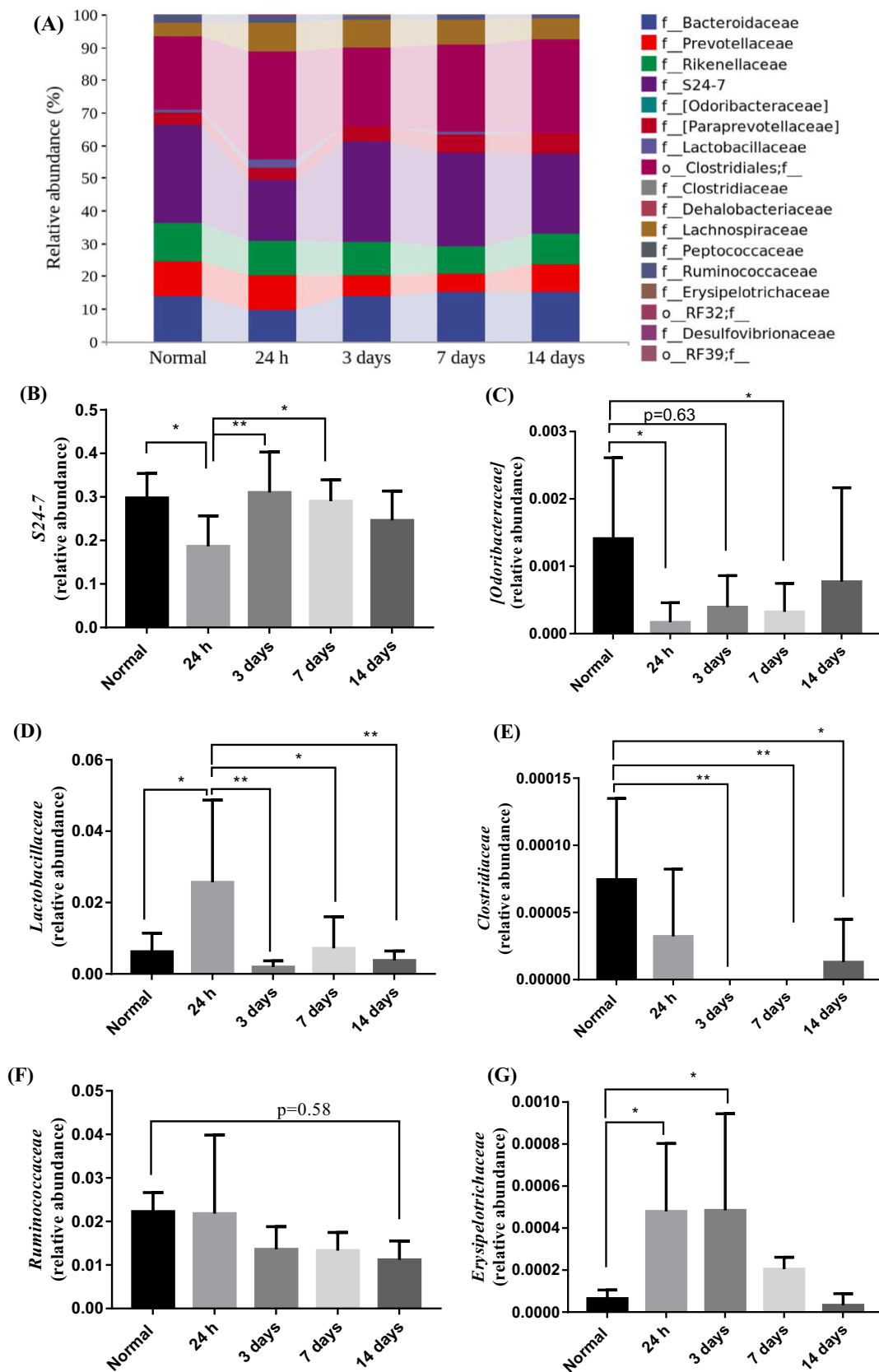


Fig. 9. Fecal microbiota composition at family level (A) and differences of bacterial relative abundance among 5 groups (B-G), n = 5. Data is shown as mean ± SD. * p < 0.05 and ** p < 0.01 are taken as significant and extremely significant, respectively. [Odoribacteraceae] is Bacteroidales_[Odoribacteraceae].

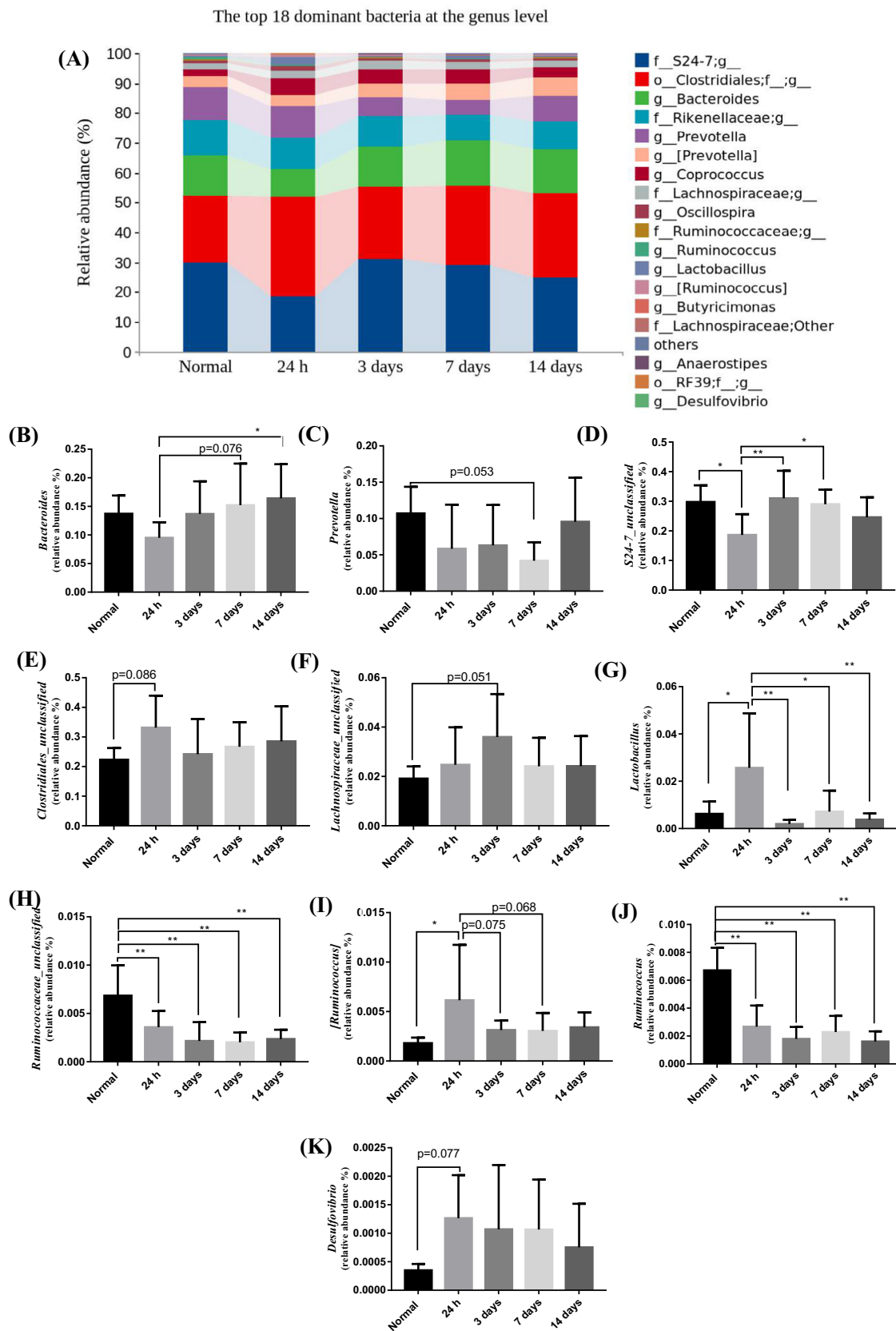


Fig. 10. The top 18 dominant bacteria at genus level (A) and differences of bacterial relative abundance among 5 groups (B–K), $n = 5$. Data is shown as mean \pm SD. * $p < 0.05$ and ** $p < 0.01$ are taken as significant and extremely significant, respectively. *[Ruminococcus]* is *Lachnospiraceae_Ruminococcus*. *[Prevotella]* is *Bacteroidales_Paraprevotellaceae_Prevotella*.

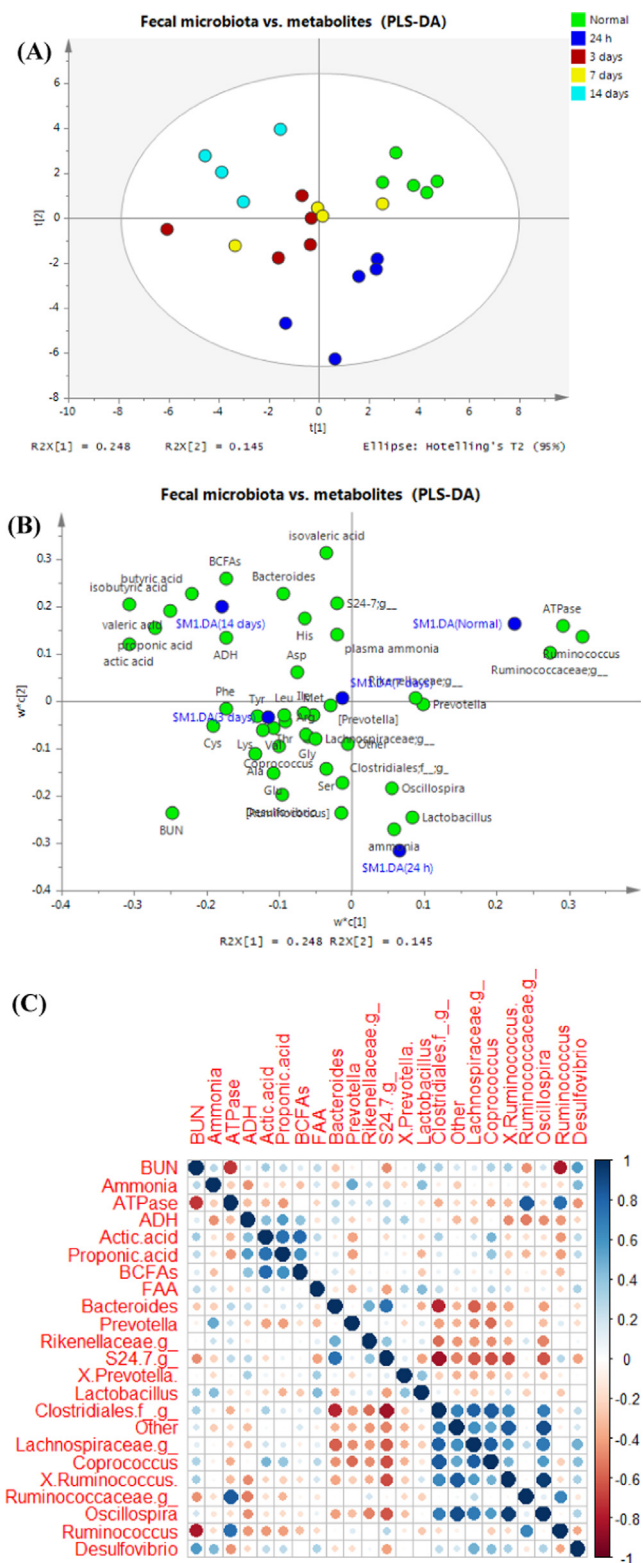


Fig. 11. Score scatter plot displays location of mice in the Normal, 24 h, 3 days, 7 days and 14 days exposure to high RH groups (A). $n = 5$, each circle represents one mouse. For the 7 days and 14 days groups, one outlier exists in each of the two groups and is not shown here. Loading scatter plot (B) shows connections between the fecal microbiota at genus level and plasma parameters (BUN, ADH, ammonia and erythrocyte Na^+/K^+ -ATPase activity) and feces (FAAs and SCFAs). Microbial taxa are represented as green circles and each blue circle represented one group. Correlation analysis based on those parameters was calculated and visualized by R3.6.0 (C). The blue circles represent positive correlation, red circles represent negative correlation, and the size and shade of the circles represent the degree of correlation. Abbreviations: RH, relative humidity; ADH, antidiuretic hormone; BUN, Blood Urea Nitrogen; FAAs, free amino acids; SCFAs, short-chain fatty acids; BCFAs, branched-chain fatty acids.

(Fig. 10 A). In the 24 h group, *Lactobacillus* ($p < 0.05$), *Lachnospiraceae_Ruminococcus* ($p < 0.05$), *Desulfovibrio* ($p = 0.077$) and *Clostridiales_unclassified* ($p = 0.086$) were highly enriched, while *S24-7_unclassified* ($p < 0.05$), *Ruminococcus* ($p < 0.01$) and *Ruminococcaceae_unclassified* ($p < 0.01$) were in significantly low abundance relative to the Normal group (Fig. 10 G-K). On the contrary, compared with the 24 h group, the relative abundance of *Lactobacillus* and *Lachnospiraceae_Ruminococcus* was lower, while the abundance of *S24-7_unclassified* was higher in other high RH exposure groups. The relative abundance of genus *Bacteroides* tended to be increased in the 7 days group ($p = 0.076$) and showed good enrichment in the 14 days group ($p < 0.05$, Fig. 10 B). The relative abundances of *Ruminococcus* ($p < 0.01$) and *Ruminococcaceae_unclassified* ($p < 0.01$) were lower in all high RH exposure groups compared to the Normal group. Meanwhile, the relative abundance of genus *Prevotella* in the 7 days group tended to decrease ($p = 0.053$) relative to the Normal group (Fig. 10 C).

Multivariate analysis

Based on fecal microbiota data at genus level and variables, an overview of the relationships among various groups is shown in Fig. 11. In the score scatter plot (Fig. 11 A), different groups are separated into different areas. The 24 h group is located between the Normal and the 7 days group. The 14 days group is associated with increased levels of SCFAs, plasma BUN, and ADH, as well as showed enriched abundance of *Bacteroides*. The 3 days group is like the 7 days group, showing association with increased fecal free amino acids and enriched abundances of *S24-7_unclassified* and *Desulfovibrio*. In contrast, these were lower in the Normal group, as shown in the opposite direction in the loading scatter plot. Here, erythrocyte Na^+/K^+ -ATPase activity was higher along with increased abundances of family *Ruminococcaceae*, including *Ruminococcus* and *Ruminococcaceae_unclassified* (Fig. 11 B). Furthermore, Pearson correlation analysis revealed that the plasma BUN level was highly negatively correlated with erythrocyte Na^+/K^+ -ATPase activity ($r = -0.71$, $p < 0.01$) and the abundance of *Ruminococcaceae_unclassified* ($r = -0.45$, $p < 0.05$). Whereas, the plasma ADH level was highly negatively correlated with erythrocyte Na^+/K^+ -ATPase activity ($r = -0.31$, $p < 0.05$) and colonic ammonia ($r = -0.46$, $p < 0.05$). Notably, the erythrocyte Na^+/K^+ -ATPase activity was highly positively correlated with the abundance of *Ruminococcaceae_unclassified* ($r = 0.83$, $p < 0.01$). The plasma BUN was highly positively correlated with the abundance of *Desulfovibrio* ($r = 0.57$, $p < 0.01$), while highly negatively correlated with the abundance of *Ruminococcus* ($r = -0.81$, $p < 0.01$) (Fig. 11 C).

Discussion

Chen *et al.* [23] revealed that exposure to high humidity (85 ~ 90%, 12 h per day) led to gut microbiota dysbiosis in a mice model; however, the gut-microbiota related alteration of intestinal metabolism remained unclear. In this study, preliminary findings suggested that exposure to high RH increased blood BUN levels in a mice model. This promoted the level of urea in the colon consequently affecting the colonic urea-nitrogen metabolism potentially by changing gut microbiota composition/activity. Based on our findings we suggest the following mechanism (Fig. 12): short-term high RH ($90 \pm 2\%$) exposure quickly reduced the erythrocyte Na^+/K^+ -ATPase activity in mice, inducing lower plasma osmolality. This may regulates ADH secretion and changing the urea retention in the body. Consequently, the colonic urea-nitrogen metabolism might get influenced by an increase in urea flux and by an altered gut microbiota composition/activity during the exposure. Such a change plays a critical role in colonic nitrogen flux metabolism involving urea degradation, amino acid synthesis, and SCFAs synthesis [10].

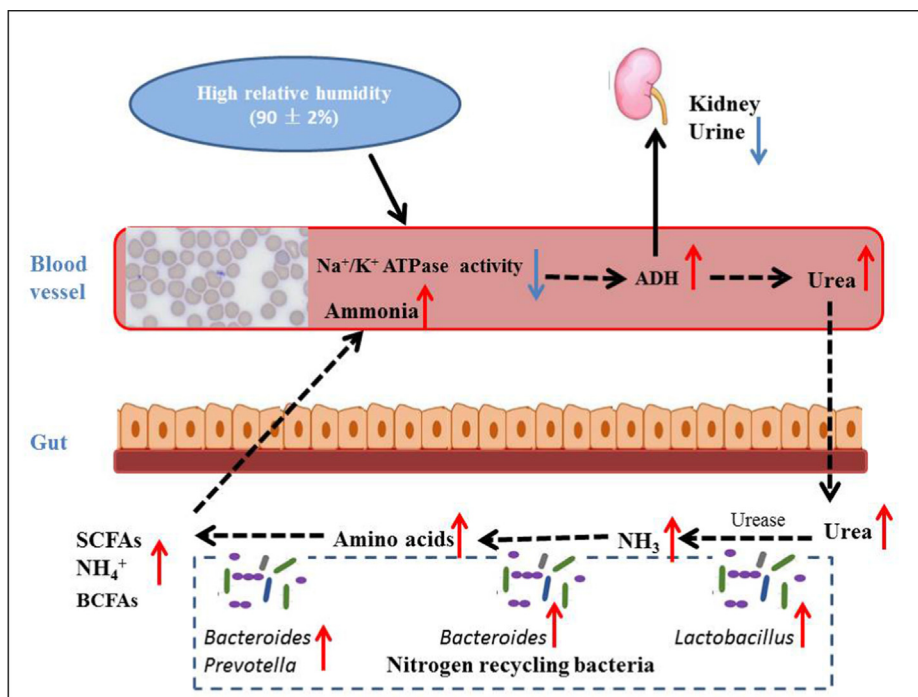


Fig. 12. Schematic representation of colonic urea-nitrogen metabolism in mice exposed to high RH.

Excess urea into the colon might impact the colonic urea-nitrogen metabolism involving intestinal microbiota

The standard human diet contains about 85 g protein per day, which is equal to about 13.6 g N or 1 M N per 70 kg body weight per day [29]. Urea, a nitrogenous waste product formed during the catabolism of dietary protein, is excreted through the urine (~82%), sweat (~3%), or gets delivered into the colon (~15%) [10,29,30]. The comparable studies in sheep and rabbits revealed that 27 ~ 30% of cecal ammonia is endogenously derived from urea [31]. Therefore, it is suggested that too much endogenous urea might flow into the colon, eventually producing ammonia with the aid of urease. This changes the intestinal environmental homeostasis by increasing the pH causing negative impacts on host health [32]. The current study indicated that plasma BUN levels were significantly increased in mice exposed to high RH for 12 h, inducing an increase in colonic urea flux. Eventually, after 24 h, increased ammonia content in the colon raised the fecal pH [33]. The reduction in colonic BUN level could be due to colonic urea hydrolysis into carbon dioxide and ammonia by bacterial urease [10]. Ammonia stress has been associated with an increase in the relative abundance of Firmicutes bacteria [34]. Notably, *Lactobacillaceae* abundance was found to be positively correlated with ammonia-N levels [35]. A similar change in relative abundance of these microbes was seen in the 24 h group of the current study, with an increase in colonic ammonia level, but not the colonic BUN level. However, after 24 h, the colonic ammonia level was not increased along with the increasing of colonic BUN level. It could be possible that the high level of ammonia gets instantly converted into other microbial metabolites. Besides, the genus *Lactobacillus*, one of the major acid ureases producer in the gut [36], was enriched in the 24 h group. This further confirms that 24-hour high RH exposure increased urea flow into the colon and thereby was used as substrate for urease related bacteria, e.g., family *Lactobacillaceae* and genus *Lactobacillus*.

Notably, the gut microbiota can rapidly consume urea-derived ammonia as the nitrogen source [37] for the biosynthesis of various amino acids, such as glutamate, glutamine, asparagine, valine, leucine, isoleucine, phenylalanine, tryptophan, and tyrosine [20]. Earlier, compared with germ-free mice, in the gastrointestinal tract

of conventionalized mice, the distribution of free amino acids was significantly altered indicating a major role of gut microbiota in amino acid homeostasis and host health [38]. Notably, we found the relative abundance of genus *Bacteroides*, an important bacteria in colonic amino acid metabolism [39], was significantly higher in the 7 days ($p = 0.076$) and 14 days groups ($p < 0.05$) relative to the 24 h group, but not to the Normal group. This suggests that the genus related to amino acid metabolism could get altered during the exposure.

Many studies showed that gut amino acids can be utilized for the biosynthesis of SCFAs via deamination, involving gut microbiota [10,40,41]. Besides, certain toxic products, such as amines, phenols/indoles, and sulfurous compounds, are also produced during the biosynthesis [41]. Meanwhile, the gut bacteria can rapidly assimilate ammonia (as a nitrogen source) into the microbial amino acids biosynthesis [20]. The gut microbiota of the mice subtly completes the colonic urea-nitrogen metabolism process, from urea to ammonia, amino acids, and lastly to SCFAs. Specifically, bacterial fermentation of glycine, alanine, threonine, glutamate, lysine, and aspartate can produce acetate; bacterial fermentation of threonine, glutamate, and lysine can produce butyrate, and alanine and threonine can produce propionate [39]. Fascinatingly, all these contents increased after 7-day exposure, while reduced in the 14 days group. The relative abundance of genus *Prevotella*, a producer of acetic, lactic, and succinic acids as the major metabolic end products, was relatively higher in the 14 days group than in the 7 days group [42], and this significantly raised the SCFAs level. Moreover, we found that the plasma BUN levels were highly negatively correlated with the abundance of *Ruminococcaceae_unclassified*, which are commonly found in the mammal intestines and can break down plant material such as cellulose and hemicellulose [43]. A lower abundance of *Ruminococcaceae_unclassified* indicates that the gut digestive function gets affected by high RH exposure, which is also reflected as the changes in the fecal appearance. Taken together, short-term exposure to high RH could induce abnormal nitrogen flux metabolism involving intestinal bacteria.

So far, only a few studies have examined the influence of high RH on health. Based on our findings using a high RH exposure model, more in-depth investigations must be carried out to examine the potential roles of gut microbiota and its end products in

amino acid and SCFAs perturbations, affecting host health. The changes in fecal microbiota composition, such as an increase in Firmicutes versus Bacteroidetes ratios and almost complete omission of Verrucomicrobia phylum, favors enhanced energy extraction [44]. We noticed that during the high RH exposure, the Firmicutes versus Bacteroidetes ratio increased after 24 h, and then reduced to the Normal group level after 3 days until 14 days. This indicates that the change in fecal microbiota composition might be involved in energy homeostasis. Furthermore, during high RH exposure, the increased content of SCFAs (acetate, propionate, butyrate) can be absorbed in the lower gut to harvest energy [45]. The bacterial metabolites, e.g., SCFAs and amino acids, mediates a critical role in host physiology [46]. The increased production of acetate in the 7 days and 14 days groups could have activated the parasympathetic nervous system to promote hyperphagia [47]. However, the effect of acetate on glucose-stimulated insulin secretion, ghrelin secretion, obesity and related sequelae [47] did not determined in the current study. Notably, 7-day and 14-day duration of high RH exposure increased the colonic amino acids and SCFAs contents. Meanwhile, some toxic compounds, such as amines, phenols/indoles, sulfurous compounds along with BCFAs were also produced as end-products [20]. Our results show that the BCFAs content, used as a biomarker of protein catabolism [21], was significantly higher in the 14 days group. Although little is known about the impact of BCFAs on host health, the negative impacts of pro-inflammatory, cytotoxic, and neuroactive compounds produced from the sulfur-containing, basic and aromatic amino acids has been confirmed [40]. Also, the higher plasma ammonia content found in the 14 days group, compared to the 12 h group, could have mainly arrived from deamination during the SCFAs synthesis in the gut, increasing the incidence of hyperammonemia [29]. Therefore, other metabolites, including phenols/indoles, sulfurous compounds, also should be studied deeply to investigate the overall impact of colonic urea-nitrogen metabolites on host health.

High relative humidity exposure reduces Na^+/K^+ -ATPase activity and damages erythrocytes

In addition to the change in the colonic urea-nitrogen cycle, we found that high humidity exposure significantly decreased the erythrocyte Na^+/K^+ -ATPase activity in mice. Moreover, this change was negatively correlated with the plasma BUN levels. Na^+/K^+ -ATPase, also called the sodium pump, is an ion transporter that exports three Na^+ ions and imports two K^+ ions across the plasma membrane by hydrolyzing ATP [48,49]. It is a ubiquitously expressed membrane-bound enzyme in the plasma membrane of all animal cells regulating membrane potential, cellular volume, and neuronal communication [50]. In the case of reduced activity of the sodium pump, a decrease in plasma osmolarity reduces sodium content in the erythrocyte. Besides, hyponatremia may be caused by increased secretion of antidiuretic hormone [51], causing urea retention in the body.

An altered activity of erythrocyte Na^+/K^+ -ATPase can disrupt the cell membrane of red blood cells [52]. Due to decreased erythrocyte Na^+/K^+ -ATPase activity, abnormal erythrocyte morphologies appeared in the 3, 7 and 14 days groups, showing bigger size, deformed shape, bite cells, burr cells, and teardrop cells. Burr cells have also been noticed in the case of changed intravascular fluid tonicity, e.g., azotemia [24]. This is consistent with our results as the plasmas ammonia content increased significantly after 14-day exposure compared to the 12 h group. Erythrocytes, the most abundant cells in the blood, deliver oxygen to tissues and organs [53] and are involved in immune function [54]. The erythrocytes with damaged structures may fail to perform immune function. Moreover, the microbiota plays a fundamental role in the induction, training, and function of the host immune system [55]. For instance, changes in Firmicutes versus Bacteroidetes ratio, observed in high RH exposure groups, have been associated with

inflammatory diseases, such as obesity and diabetes [56]. Gao *et al.* reported that the short-duration exposure (~68% relative humidity, 28 days) was associated with altered levels of CD8 + T cells, indicating that even a short-term humid environment can influence human immune profiles [57]. In this study, though the erythrocytes morphologies were found to be abnormal, their role in influencing the immune function, the cross-talk between host immune and gut microbiota, including the effects on gut microbiota metabolites needs to be further investigated.

Conclusion

In this study, short-term high RH exposure resulted in abnormal erythrocyte morphologies and affecting colonic urea-nitrogen metabolism by changing gut microbiota. Plasma BUN retention markedly responded to the high RH exposure, along with decreased erythrocyte Na^+/K^+ -ATPase activity and up-regulation of ADH secretion. The excessive accumulated BUN enters the colon and thus changes the gut microbiota composition. This further disorders the levels of ammonia, amino acids, and SCFAs. Further, the products of colonic urea-nitrogen metabolism, e.g., acetate, ammonia, and BCFAs, might induce hyperphagia, hyperammonemia, immune dysfunction, and other health issues. Overall, these findings can be explored further to understand the influence of high RH exposure on human health.

Ethical statement

All Institutional and National Guidelines for the care and use of animals (mice) were followed. All animals used in this study were cared for in accordance with the Guidelines for the Care and Use of Laboratory Animals published by the United States National Institute of Health (NIH, Publication No. 85–23, 1996), and all procedures were approved by the Animal Care Review Committee (Animal application approval number 0064257), Nanchang University, China.

CRedit authorship contribution statement

Hongmei Yin: Conceptualization, Investigation, Formal analysis, Writing - original draft. **Yadong Zhong:** Conceptualization, Methodology, Writing - review & editing. **Hui Wang:** Conceptualization, Investigation. **Jielun Hu:** Writing - review & editing, Funding acquisition. **Shengkun Xia:** Investigation. **Yuandong Xiao:** Resources. **Shaoping Nie:** Supervision. **Mingyong Xie:** Supervision, Conceptualization, Funding acquisition.

Declaration of Competing Interest

The authors have declared no conflict of interest.

Acknowledgments

Chinese Academy of Food Science and Technology-Jiangzhong Gastrointestinal Health Special Fund (2019-05), The National Key Research and Development Program of China (2017YFC1600405), Jiangxi Provincial Major Program of Research and Development Foundation (Agriculture field) (20165ABC28004), The National Natural Science Foundation of China (31571826; 31770861; 31960464), Construction of Science and Technology Innovation Platform base in Jiangxi Province (2020ZDZH02058), are gratefully acknowledged.

References

- [1] Davis RE, McGregor GR, Enfield KB. Humidity: A review and primer on atmospheric moisture and human health. *Environ Res* 2016;144:106–16.

- [2] Goggins WB, Woo J, Ho S, Chan EY, Chau P. Weather, season, and daily stroke admissions in Hong Kong. *Int J Biometeorol* 2012;56(5):865–72.
- [3] Vaneckova P, Neville G, Tippett V, Aitken P, FitzGerald G, Tong S. Do biometeorological indices improve modeling outcomes of heat-related mortality?. *J Appl Meteorol Clim* 2011;50(6):1165–76.
- [4] Barnett AG, Tong S, Clements AC. What measure of temperature is the best predictor of mortality?. *Environ Res* 2010;110(6):604–11.
- [5] Montero JC, Mirón JJ, Criado-Álvarez JJ, Linares C, Díaz J. Influence of local factors in the relationship between mortality and heat waves: Castile-La Mancha (1975–2003). *Sci Total Environ* 2012;414:73–80.
- [6] Barreca AI. Climate change, humidity, and mortality in the United States. *J Environ Econ Manag* 2012;63(1):19–34.
- [7] Jin L, Zhang Y, Zhang Z. Human responses to high humidity in elevated temperatures for people in hot-humid climates. *Build Environ* 2017;114:257–66.
- [8] Fan X, Liu W, Wargocki P. Physiological and psychological reactions of sub-tropically acclimatized subjects exposed to different indoor temperatures at a relative humidity of 70%. *Indoor Air* 2019;29(2):215–30.
- [9] Human Microbiome Project C. Structure, function and diversity of the healthy human microbiome. *Nature* 2012;486(7402):207–214.
- [10] Ni J, Shen TCD, Chen EZ, Bittinger K, Bailey A, Roggiani M, et al. A role for bacterial urease in gut dysbiosis and Crohn's disease. *Sci Transl Med* 2017;9(416). eah6888.
- [11] Tilg H, Zmora N, Adolph TE, Elinav E. The intestinal microbiota fuelling metabolic inflammation. *Nat Rev Immunol* 2020;20:40–54.
- [12] Abdel-Daim MM, Farouk SM, Madkour FF, Azab SS. Anti-inflammatory and immunomodulatory effects of *Spirulina platensis* in comparison to Dunalialia salina in acetic acid-induced rat experimental colitis. *Immunopharm Immunot* 2015;37(2):126–39.
- [13] Euony OI, Eblehi SS, Avdek-Latif HM, Abdel-Daim MM, Ei-Sayed YS. Modulatory role of dietary *Thymus vulgaris* essential oil and *Bacillus subtilis* against thiamethoxam-induced hepatorenal damage, oxidative stress, and immunotoxicity in African catfish (*Clarias garipenus*). *Environ Sci Pollut Res* 2020;27:23108–28.
- [14] Jian XX, Zhu YH, Ouyang J, Wang YH, Lei Q, Xia JL, et al. Alterations of gut microbiome accelerate multiple myeloma progression by increasing the relative abundances of nitrogen-recycling bacteria. *Microbiome* 2020;8:74.
- [15] Chako A, Cummings JH. Nitrogen losses from the human small bowel: obligatory losses and the effect of the physical form of food. *Gut* 1988;29:809–15.
- [16] Stewart GS, Fenton RA, Thévenod F, Smith CP. Urea movement across mice colonic plasma membranes is mediated by UT-A urea transporters. *Gastroenterology* 2004;126:765–73.
- [17] Visek WJ. Diet and cell growth modulation by ammonia. *Am J Clin Nutr* 1978;10.
- [18] Metges CC. Contribution of microbial amino acids to amino acid homeostasis of the host. *J Nutr* 2000;130:1857S–64S.
- [19] Fan P, Li L, Rezaei A, Eslamfam S, Che D, Ma X. Metabolites of dietary protein and peptides by intestinal microbes and their impacts on gut. *Curr Protein Pept Sci* 2015;16:646–54.
- [20] Portune KJ, Beaumont M, Davila A-M, Tomé D, Blachier F, Sanz Y. Gut microbiota role in dietary protein metabolism and health-related outcomes: The two sides of the coin. *Trends Food Sci Tech* 2016;57:213–32.
- [21] Yao CK, Muir JG, Gibson PR. Review article: insights into colonic protein fermentation, its modulation and potential health implications. *Aliment Pharm Ther* 2016;43(2):181–96.
- [22] Taketo O, Mitsuru K, Yuko K, Masahito T, Toshihisa S, Kohzo T. Effects of high ambient temperature on urea-nitrogen recycling in lactating dairy cows. *Anim Sci J* 2011:531–6.
- [23] Chen S, Zheng Y, Zhou Y, Guo W, Tang Q, Rong G, et al. Gut Dysbiosis with Minimal Enteritis Induced by High Temperature and Humidity. *Sci Rep* 2019;9(1):18686.
- [24] Xiao Y, Xiong T, Peng Z, Liu C, Huang T, Yu H, et al. Correlation between microbiota and flavours in fermentation of Chinese Sichuan Paocai. *Food Res Int* 2018;114:123–32.
- [25] Hu JL, Nie SP, Min FF, Xie MY. Polysaccharide from seeds of *Plantago asiatica* L. increases short-chain fatty acid production and fecal moisture along with lowering pH in mice colon. *J Agr Food Chem* 2012;60(46):11525–32.
- [26] García-García N, Tamames J, Linz AM, Pedrós-Alió C, Puente-Sánchez F. Microdiversity ensures the maintenance of functional microbial communities under changing environmental conditions. *Isme J* 2019;13:2969.
- [27] Caporaso JG, Kuczynski J, Stombaugh J, Bittinger K, et al. QIIME allows analysis of high-throughput community sequencing data. *Nat Methods* 2010. doi: <https://doi.org/10.1038/nmeth.1303>.
- [28] Jones KW. Evaluation of cell morphology and introduction to platelet and white blood cell morphology. *Clinical hematology fundamentals hemostasis* 2009:93–116.
- [29] Levitt D, Levitt M. A model of blood-ammonia homeostasis based on a quantitative analysis of nitrogen metabolism in the multiple organs involved in the production, catabolism, and excretion of ammonia in humans. *Clin Exp Gastroenterol* 2018;11:193–215.
- [30] Dunstan RH, Sparkes DL, Dascombe BJ, Macdonald MM, Evans CA, Stevens CJ, et al. Sweat facilitated amino acid losses in male athletes during exercise at 32–34°C. *PLoS ONE* 2016;11(12). e0167844.
- [31] Ouellet DR, Berthiaume R, Holtrop G, Lobley GE, Martineau R, Lapierre H. Effect of method of conservation of timothy on endogenous nitrogen flows in lactating dairy cows. *J Dairy Sci* 2010;93(9):4252–61.
- [32] Lin HC, Visek WJ. Large Intestinal pH and Ammonia in Rats: Dietary Fat and Protein Interactions. *J Nutr* 1991;121(6):832–43.
- [33] Blachier F, Beaumont M, Andriamihaja M, Davila A-M, Lan A, Grauso M, et al. Changes in the Luminal Environment of the Colonic Epithelial Cells and Physiopathological Consequences. *Am J Pathol* 2017;187(3):476–86.
- [34] Gao S, Zhao M, Chen Y, Yu M, Ruan W. Tolerance response to in situ ammonia stress in a pilot-scale anaerobic digestion reactor for alleviating ammonia inhibition. *Bioresour Technol* 2015;198:372–9.
- [35] Ren FY, He RC, Zhou XK, Gu QC, Xia ZS, Liang MZ, et al. Dynamic changes in fermentation profiles and bacterial community composition during sugarcane top silage fermentation: A preliminary study. *Bioresour Technol* 2019;285:121315.
- [36] Kakimoto S, Miyashita H, Sumino Y, Akiyama S. Properties of Acid Ureas from *Lactobacillus* and *Streptococcus* Strains. *Agri Biol Chem* 1990;54(2):381–6.
- [37] Magasanik B. The regulation of nitrogen utilization in enteric bacteria. *J Cell Biochem* 1993;51(1):34–40.
- [38] Mardinoglu A, Shoaie M, Bergentall P, Ghaffari C, Zhang C, Larsson E, et al. The gut microbiota modulates host amino acid and glutathione metabolism in mice. *Mol Syst Biol* 2015;11(834):1–15.
- [39] Dai ZL, Wu G, Zhu WY. Amino acid metabolism in intestinal bacteria: links between gut ecology and host health. *Frontiers in bioscience : a journal and virtual library* 2011;16:1768–86.
- [40] Oliphant K, Allen-Vercoe E. Macronutrient metabolism by the human gut microbiome: major fermentation by-products and their impact on host health. *Microbiome* 2019;7(1):91.
- [41] Davila AM, Blachier F, Gotteland M, Andriamihaja M, Benetti PH, Sanz Y, et al. Intestinal luminal nitrogen metabolism: Role of the gut microbiota and consequences for the host. *Pharmacol Res* 2013;68(1):95–107.
- [42] Alauzet C, Mory F, Carlier JP, Marchandin H, Jumas-Bilak E, Lozniewski A. *Prevotella nanceiensis* sp. nov., isolated from human clinical samples. *Int J Syst Evol Micr* 2007;10(57):2216–20.
- [43] Kim HN, Joo EJ, Cheong HS, Kim Y, Kim HL, Shin H, et al. Gut Microbiota and Risk of Persistent Nonalcoholic Fatty Liver Diseases. *J Clin Med* 2019;8(8):1089.
- [44] Chevalier C, Stojanović O, Colin DJ, Suarez-Zamorano N, Tarallo V, Veyrat-Durebex C, et al. Gut Microbiota Orchestrates Energy Homeostasis during Cold. *Cell* 2015;163(6):1360–74.
- [45] Delzenne NM, Cani PD. Gut Microbiota and the Pathogenesis of Insulin Resistance. *Curr Diab Rep* 2011;11:154–9.
- [46] Sridharan GV, Choi K, Klemashevich C, Wu C, Prabakaran D, Pan LB, et al. Prediction and quantification of bioactive microbiota metabolites in the mice gut. *Nat Commun* 2014;5(1):5492.
- [47] Perry RJ, Peng L, Barry NA, Cline GW, Zhang DY, Cardone RL, et al. Acetate mediates a microbiome-brain-β-cell axis to promote metabolic syndrome. *Nature* 2016;534:213–7.
- [48] Chen Y, Cai T, Wang H, Li Z, Loreaux E, Lingrel JB, et al. Regulation of intracellular cholesterol distribution by Na/K-ATPase. *J Biol Chem* 2009;284(22):14881–90.
- [49] Qu F, Liu S, He C, Zhou J, Zhang S, Ai Z, et al. Comparison of the Effects of Green and Black Tea Extracts on Na⁺/K⁺-ATPase Activity in Intestine of Type 1 and Type 2 Diabetic Mice. *Mol Nutr Food Res* 2019;63(17):e1801039.
- [50] Mobasheri A, Avila J, Cózar-Castellano I, Brownleader MD, Trevan M, Francis MJ, et al. Na⁺, K⁺-ATPase isozyme diversity; comparative biochemistry and physiological implications of novel functional interactions. *Bioscience Rep* 2000;20(2):51–91.
- [51] Kawaguchi T, Takeuchi M, Kawajiri C, Abe D, Nagao Y, Yamazaki A, et al. Severe hyponatremia caused by syndrome of inappropriate secretion of antidiuretic hormone developed as initial manifestation of human herpesvirus-6-associated acute limbic encephalitis after unrelated bone marrow transplantation. *Transpl Infect Dis* 2013;15(2):E54–7.
- [52] Omar AK, Ahmed KA, Helmi NM, Abdullah KT, Qarii MH, Hasan HE, et al. The sensitivity of Na⁺, K⁺ATPase as an indicator of blood diseases. *Afr Health Sci* 2017;17(1):262–9.
- [53] Zhang J, Wang P, Xu F, Huang W, Ji Q, Han Y, et al. Protective effects of lycopene against AFB1-induced erythrocyte dysfunction and oxidative stress in mice. *Res Vet Sci* 2020;129:103–8.
- [54] Siegel I, Lin TL, Gleicher N. The red-cell immune system. *The Lancet* 1981;318(8246):556–9.
- [55] Belkaid Y, Hand TW. Role of the microbiota in immunity and inflammation. *Cell* 2014;157:121–41.
- [56] Lindenberg F, Krych L, Fielden J, et al. Expression of immune regulatory genes correlate with the abundance of specific Clostridiales and Verrucomicrobia species in the equine ileum and cecum. *Sci Rep* 2019;9:12674.
- [57] Gao X, Colicino E, Shen J, Kioumourtzoglou MA, Just AC, Nwanjiri-Enwerem JC, et al. Impacts of air pollution, temperature, and relative humidity on leukocyte distribution: An epigenetic perspective. *Environ Int* 2019;126:395–405.